HHS Public Access

Author manuscript

Bone. Author manuscript; available in PMC 2023 April 10.

Published in final edited form as:

Bone. 2022 April ; 157: 116310. doi:10.1016/j.bone.2021.116310.

Deletion of *IL-17ra* in osteoclast precursors increases bone mass by decreasing osteoclast precursor abundance

Joseph L. Roberts[a,b], **Giovanni Mella-Velazquez**[a], **Hamid Y. Dar**[a,b], **Guanglu Liu**[b], **Hicham Drissi**[a,b,*]

[a]Department of Orthopaedics, Emory University School of Medicine, Atlanta, GA, USA

[b]The Atlanta Department of Veterans Affairs Medical Center, Decatur, GA, USA

Abstract

Metabolic bone diseases, such as osteoporosis, typically reflect an increase in the number and activity of bone-resorbing osteoclasts that result in a loss of bone mass. Inflammatory mediators have been identified as drivers of both osteoclast formation and activity. The IL-17 family of inflammatory cytokines has gained attention as important contributors to both bone formation and resorption. The majority of IL-17 cytokines signal through receptor complexes containing IL-17a receptor (IL-17ra); however, the role of IL-17ra signaling in osteoclasts remains elusive. In this study, we conditionally deleted IL-17ra in osteoclast precursors using *LysM-Cre* and evaluated the phenotypes of skeletally mature male and female conditional knockout and control mice. The conditional knockout mice displayed an increase in trabecular bone microarchitecture in both the appendicular and axial skeleton. Assessment of osteoclast formation *in vitro* revealed that deletion of IL-17ra decreased osteoclast number, which was confirmed *in vivo* using histomorphometry. This phenotype was likely driven by a lower abundance of osteoclast precursors in IL-17ra conditional knockout mice. This study suggests that IL-17ra signaling in preosteoclasts can contribute to osteoclast formation and subsequent bone loss.

Keywords

inflammation; bone turnover; bone resorption; IL-17a; cytokine

1. Introduction

The number and degree of osteoclast activity are strong determinants of the quality and quantity of bone. Virtually all metabolic bone diseases reflect increased bone resorption relative to bone formation. Thus, precise regulation of both osteoclast formation and activity

*Address correspondence to: Hicham Drissi, PhD, Department of Orthopaedics, Emory University School of Medicine, Atlanta, GA, USA, hicham.drissi@emory.edu.

Author contributions: J.L.R. and H.D. designed the study. J.L.R., G.M.V., H.Y.D., and G.L. performed the experiments. J.L.R., G.M.V., and H.Y.D. analyzed the results. J.L.R. drafted the manuscript. All authors have read and approved the final submitted manuscript.

is critical to maintaining bone mass. Under homeostatic conditions these processes are tightly controlled by many factors, including hormones (e.g., PTH, estrogen) and locally secreted molecules (e.g., Wnt5a, RANKL) (1–4). Inflammatory cytokines have also been shown to control osteoclastogenesis (5–8). This is especially obvious in inflammatory bone diseases like periarticular osteolysis that accompanies rheumatoid arthritis. In these diseases, cytokines including TNF-α and IL-1 can synergize to potently stimulate osteoclastogenesis (9, 10). More recently, IL-17a has emerged as an important contributor to inflammatory bone loss (11).

Traditionally, it is thought that IL-17a indirectly stimulates osteoclastogenesis through osteoblasts (12). In this model, binding of IL-17a to its ubiquitously expressed receptor, IL-17ra, on osteoblasts stimulates the expression and secretion of RANKL and M-CSF (12). However, mounting evidence points to a more direct role of IL-17a control of osteoclastogenesis by priming osteoclast precursors to commit to the osteoclast fate through up-regulation of RANK expression (13). The expression of IL-17ra in preosteoclasts and seemingly enhanced osteoclast formation at low concentration of IL-17a further suggests a direct effect of IL-17a-IL-17ra signaling (14, 15). Importantly, IL-17ra is an obligate component of receptor complexes that mediate signaling for other IL-17 ligands, including IL-17f, IL-17e, IL-17c, and IL-17b. Thus, this study sought to determine if IL-17ra in osteoclast precursors influences osteoclast formation and, by effect, bone mass in young, unchallenged mice. We conditionally deleted IL-17ra in pre-osteoclasts using *LysM-Cre* and observed an increase in trabecular bone that stemmed from decreased osteoclasts. Furthermore, we assessment of bone marrow derived osteoclast precursor populations revealed significantly lower osteoclast precursors, which likely contributed to the observed phenotype.

2. Methods

2.1. Animal husbandry

LysM-Cre mice were from Jackson Labs. The *IL-17ra*$^{F/F}$ mice were kindly provided by Dr. Michael Karin (University of California, San Diego) and have previously been described (16). *LysM-Cre* mice were bred with the *IL-17ra*$^{F/F}$ mice to generate *LysM-Cre*;*IL-17ra*$^{F/+}$ mice, which were then crossed with *IL-17ra*$^{F/F}$ mice to generate experimental *LysM-Cre*;*IL-17ra*$^{F/F}$ (*IL-17ra* cKO) mice. Conditional knockout mice were compared to *IL-17ra*$^{F/+}$ littermate controls. All mice are in the C57BL/6 background. Ten-week-old male and female mice were used for all experiments. Mice had *ab libitum* access to autoclaved food (Envigo #2018S) and water. All mice were housed at the Atlanta Veterans Affairs Medical Center (VAMC) animal facility in specific pathogen free cages and controlled conditions (temperature, 21–24°C; humidity, 40–70%; light/dark cycle, 12/12 h). Mice were maintained in accordance with applicable state and federal guidelines and all experimental procedures were approved by the Atlanta VAMC Institutional Animal Care and Use Committee.

2.2. Micro-computed tomography

Micro-Computed tomography (μCT) was performed on the femur and 3rd lumbar (L3) vertebrae *ex vivo* to assess trabecular and cortical bone microarchitecture using a μCT40 scanner (Scanco Medical AG, Brüttisellen, Switzerland) that was calibrated weekly using a factory-supplied phantom. Bones isolated from 10-week-old male and female mice were first fixed for 1 week in 10% neutral buffered formalin at 4°C followed by scanning in PBS medium. Femur trabecular bone indices were determined from a total of 99 tomographic slices that were taken from the distal femoral metaphysis starting 0.5 mm proximal from the distal growth plate at a voxel size of 6 μm (70 kVp and 114 mA, and with 200 ms integration time). Cortical bone was quantified at the femoral mid-diaphysis from 104 tomographic slices. Projection images were reconstructed using the auto-contour function for vertebral body trabecular bone between the cranial and caudal growth plates from approximately 350 tomographic slices. Trabecular bone and cortical bone representative samples were reconstructed in 3D to generate visual representations based on mean BV/TV and cortical thickness, respectively. The following 3D indices in the defined ROI were analyzed: bone volume fraction (BV/TV, %), trabecular number (Tb.N, mm^1), trabecular thickness (Tb.Th, μm), trabecular separation (Tb.Sp, μm), bone surface density (BS/TV, mm^2/mm^3), volumetric bone mineral density (vBMD, mg HA/cm^3), cortical thickness (Ct.Th, mm), cortical porosity (Ct.Po, %), and cortical area (Ct.Ar, mm^2). All indices and units were standardized according to published guidelines (17).

2.3. Histology and static histomorphometry

Femurs from 10-week-old male mice were fixed for 1 week in 10% neutral buffered formalin at 4°C, then decalcified in 14% EDTA (pH 7.2) for at least 2 weeks before embedding in paraffin. Five micrometer thick sections were obtained and stained for TRAP (Kamiya Biomedical Company #KT-008). We analyzed two sections in the sagittal plane from each bone using a 600 μm wide region of interest that begins 200 μm distal to the growth plate. This region of interest encompasses the secondary spongiosa quantified by micro-CT. The number of TRAP+ osteoclasts per bone perimeter and osteoclast surface per bone surface were determined using Osteomeasure (Osteometrics).

2.4. Bone marrow macrophage (BMM) osteoclast formation assay

Whole bone marrow from 10-week old experimental *LysM-Cre*;*IL-17ra*$^{F/F}$ and control mice were isolated from the long bones (i.e., femur and tibia) by flushing the medullary cavity with medium. Red blood cells were removed using RBC Lysis Buffer (Invitrogen) and remaining cells were expanded for 3 days in the presence of recombinant murine M-CSF (30 ng/mL; Peprotech; #315–02) at 37°C in 5% CO_2. Expanded BMMs were then seeded at a density of 1.5×10^4 cells/well of a 48-well plate and cultured in alpha-MEM medium (Gibco), supplemented with 10% FBS (Atlanta Biologicals), 1% penicillin-streptomycin (Gibco), and either 25 ng/mL recombinant murine M-CSF (Peprotech; #315–02) alone or recombinant murine M-CSF (25 ng/mL) and 50 ng/mL recombinant murine sRANKL (R&D Systems; #462-TEC). Media was refreshed every other day. The cells were stained with TRAP (Sigma) and the number of TRAP+ mature osteoclasts (≥3 nuclei) per well were

quantified after 3 and 5 days of culture. No distinction was made between large and small osteoclasts. Three wells per biological replicate were used for osteoclast formation assays.

2.5. Gene expression

Isolated BMMs were seeded at a density of 8×10^4 cells/well of a 24-well plate and in the presence of either 30 ng/mL M-CSF (Peprotech; #315–02) alone or M-CSF (30 ng/mL) and 50 ng/mL sRANKL (R&D Systems; #462-TEC) for 3 and 5 days at 37°C in 5% CO_2. Total RNA was isolated from cells using TRIzol (Invitrogen) according to the manufacturer's instructions. First-strand cDNA was synthesized with oligo(dT) and random primers using qScript cDNA SuperMix (Quantabio). All qRT-PCR were performed on an Analytik Jena qTower^3 G Real-Time PCR Detection System using Applied Biosystems PowerUp SYBR Green master mix. Amplicon authenticity was confirmed by melt curve analysis. Primer sequences are provided in Supplementary Table 1 and β-actin was used as the normalization control. The data were analyzed for fold change using the ΔΔCT method.

2.6. ELISA

Mice were fasted for ≥6 hours with free access to water. Whole blood was collected at time of sacrifice via cardiac puncture, allowed to clot for ≥30 minutes at room temperature, and serum isolated by centrifugation (10,000 rpm for 10 minutes). Sera was removed, aliquoted, and stored at −80°C. Carboxy-terminal collagen cross-links (CTX) (RatLaps; Immunodiagnostic Systems #AC-06F1) and IL-17a (ThermoFisher #BMS6001) were assayed using enzyme-linked immunosorbent assay kits according to manufacturer's recommendations.

2.7. Flow cytometry

Flow cytometry was performed as previously described (18, 19). Briefly, the epiphyses of long bones (tibia and femur) were cut, and bone marrow was flushed with αMEM media using a 26G needle. Single cell suspensions of bone marrow-derived cells were then prepared in αMEM media. Cells were then stained with surface markers APC/Cyanine7 anti-CD3 (clone 145–2C11, Biolegend #100330), APC anti-CD45R/B220 (clone RA3–6B2, Biolegend #103211), PE/Cyanine5 anti-CD11b (clone M1/70, Biolegend #101209), PE anti-CD115 (clone AFS98, Biolegend #135505), and FITC anti-CD117 (clone 2B8, Biolegend #105805). Zombie Red Fixable Viability Kit live/dead stain (Biolegend #423110) was used to discriminate live cells in samples. Cells were analyzed using Symphony 3 flow cytometer (BD Biosciences) and data were analyzed using FlowJo software (Tree Star, Inc., Ashland,OR).

2.8. Cell sorting and in vitro osteoclast culture

Bone marrow cells were isolated from both femurs, tibias, and pelvic bones by cutting the epiphyses, flushing the bones with αMEM media using a 26G needle, and passing through a 70μm cell strainer. Red blood cells were removed using RBC Lysis Buffer (Invitrogen). The bone marrow cells were then resuspended in αMEM media containing 10% FBS and 1% penicillin-streptomycin and kept on ice. Cells were stained for surface markers as described above (methods section 2.7.) and were sorted using a BD™ FACS

Aria II SORP. Sufficient numbers of osteoclast precursor Population VI were acquired from each mouse and were used for *in vitro* osteoclast formation assays. Equal number of cells (1.2×10^4 cells/well) were seeded in a 48-well dish in αMEM media containing 10% FBS, 1% penicillin-streptomycin, 30 ng/ml M-CSF (Peprotech; #315–02), and 50 ng/ml sRANKL (R&D Systems; #462-TEC) for 3 and 5 days at 37°C in 5% CO_2. Medium was refreshed every other day. The cells were stained with TRAP (Sigma) and the number of TRAP+ mature osteoclasts (≥3 nuclei) per well were quantified after 3 and 5 days of culture. No distinction was made between large and small osteoclasts. Two wells per biological replicate were used for osteoclast formation assays.

2.9. Statistical analysis

Results are shown as mean ± standard deviation (SD). Statistical significance was determined by unpaired two-tailed Student's *t*-test or one-way ANOVA followed by Tukey's multiple comparisons test using GraphPad Prism software (version 8.3.0). All statistical tests were performed at the 5% significance level.

3. Results

3.1. IL-17ra is highly expressed in osteoclast precursors

We first surveyed which of the known IL-17 receptors are expressed in bone marrow macrophages (BMMs) from 10-week-old control mice cultured in the presence of M-CSF for 3 days. *IL-17ra* was the most highly expressed IL-17 receptor in these cells, followed by *IL-17rd* and *IL-17rc* (Fig. 1A). We next targeted *IL-17ra* in osteoclast precursors *in vivo* by crossing *IL-17ra*$^{F/F}$ mice with *LysM-Cre* mice (Fig. 1B). This resulted in excision of exons 3 and 4 resulting in a frameshift and early termination of translation (Fig. 1B). We generated male and female mice lacking IL-17ra in osteoclast precursors, hereafter referred to as *IL-17ra* cKO, which were compared to *IL-17ra*$^{F/+}$ littermate controls. IL-17ra cKO mice developed normally, were indistinguishable from controls, and did not differ in body weight (Supplemental Figure 1). To assess the efficiency of recombination of *IL-17ra* in osteoclast precursors, BMMs were first cultured in M-CSF for 3 days. Gene expression analyses revealed a significant decrease in *IL-17ra* expression in pre-osteoclasts using primers that amplify a region of *IL-17ra* spanning exon 3 – exon 5 (deleted region) (Fig. 1C). Efficient deletion of IL-17ra was further confirmed by subjecting the PCR product to agarose gel electrophoresis, which did not produce a visible band at the expected amplicon size (Fig. 1C). We next sought to determine if IL-17ra cKO would influence systemic levels of IL-17a, the principal ligand for IL-17ra. IL-17a was detectable in the sera in both IL-17ra cKO and control mice; however, no differences in systemic IL-17a levels between genotypes in either males or females was noted (Fig. 1D).

3.2. Deletion of IL-17ra in pre-osteoclasts increases bone mass by decreasing osteoclast numbers

μCT analyses of the distal femur showed a visible increase in trabecular bone of 10-week-old male and female *IL-17ra* cKO mice (Fig. 2A). This was illustrated by a significant increase in bone volume fraction (BV/TV) and volumetric bone mineral density (vBMD), that driven by increased trabecular thickness (Tb.Th) in *IL-17ra* cKO male mice (Fig. 2A).

Similar results were also observed in the femurs of 10-week old *IL-17ra* cKO female mice, which had a significantly higher bone volume fraction (BV/TV) and volumetric bone mineral density (vBMD); however, this increase in bone was driven by a greater trabecular number (Tb.N) (Fig. 2A). In the L3 vertebral body, *IL-17ra* cKO significantly increased BV/TV, vBMD, and Tb.Th in male mice (Supplemental Fig. 2). In female mice, there was a significant increase in L3 vertebral body Tb.N in *IL-17ra* cKO mice, but BV/TV and vBMD did not differ between genotypes (Supplemental Fig. 2).

Conditional deletion of *IL-17ra* in osteoclast precursors led to a similar effect on bone in both males and females, although the effect was more prominent in male mice. Thus, we elected to process the male femurs for histological analyses (Fig. 2B). Histomorphometry of the distal femur revealed a significant increase in BV/TV in IL-17ra cKO mice (Fig. 2B). Tb.Th and Tb.N were also higher in the experimental mice although this did not reach statistical significance (Fig. 2B). No differences in Ct.Th were observed between genotypes (Fig. 2B). Together, the data indicate that conditional deletion of *IL-17ra* in osteoclast precursors increases trabecular bone microarchitectural indices in both the appendicular and axial skeleton.

The higher bone mass phenotype observed using μCT and histomorphometry suggested a possible effect of *IL-17ra* cKO on osteoclast formation or activity. Therefore, we quantified the number of TRAP+ osteoclasts within the distal femur metaphysis. There were significantly fewer osteoclasts per bone perimeter and a significant decrease in osteoclast surface over bone surface in *IL-17ra* cKO mice compared to controls (Fig. 3A). Moreover, assessment of serum CTX levels, a biomarker of bone resorption, revealed significantly lower CTX in both male and female IL-17ra cKO mice (Fig. 3B). These data suggest that the deletion of *IL-17ra* in osteoclast precursors decreases the number and activity of osteoclasts, which is likely responsible for the high bone mass phenotype observed.

3.3. Conditional deletion of IL-17ra in osteoclast precursors decreases osteoclast formation and expression of osteoclast-related genes

Activation of IL-17ra signaling in pre-osteoclasts has been suggested to directly and indirectly (through osteoblasts) promote osteoclast formation (12,13). Thus, we sought to determine if deletion in osteoclast precursors would influence osteoclast formation *in vitro* using a mixed population (unsorted) of BMMs. At day 3 of osteoclast differentiation there were significantly fewer osteoclasts in the IL-17ra cKO group (Fig. 4A). However, at day 5 no differences in osteoclast number were observed between genotypes (Fig 4A), which may be due to saturating conditions *in vitro*. Assessment of osteoclast-related genes also showed lower expression of *Ctsk*, *Calcr*, and vATPaseD2 (ATP6V0D2) at day 3 (Fig. 4B). Similarly, *Ctsk*, *Calcr*, vATPaseD2, and DC-Stamp gene expression was significantly lower in IL-17ra cKO cells at day 5 of osteoclastogenesis (Fig. 4B).

3.4. *Deletion of* IL-17ra *decreases the abundance of osteoclast precursors*

To determine a potential mechanism via which IL-17ra cKO decreases osteoclast abundance *in vitro*, we assessed the abundance of various bone marrow-derived osteoclast precursors using Flow cytometry. Previously, studies have reported that specific subsets of bone

marrow osteoclast precursors with the phenotype of CD3^{-} CD11b$^{-/low}$ CD115^{+} and either CD117^{hi}, or CD117^{low} having higher osteoclastogenic potential (18, 19). In the present study, there was significant decrease in population IV (CD3^{-} CD11b$^{-/low}$ CD117^{high}), population VI (CD3^{-} CD11b$^{-/low}$ CD117^{low}) as well as in the CD115^{+} populations in IL-17ra cKO mice (Fig. 5A&B). These data indicate that IL-17ra signaling likely contributes to osteoclastogenesis and subsequent bone turnover by influencing the abundance of osteoclast precursors.

To further confirm that the *in vitro* differences is osteoclast formation (Fig. 4A) were due to changes in osteoclast precursor abundance, we sorted bone marrow cells to isolate the most abundance osteoclast precursor population, population VI (CD3^{-} CD11b$^{-/low}$ CD117^{low}), for *in vitro* osteoclastogenesis assays. No differences in osteoclast numbers were observed at day 3 or day 5 of culture when equal numbers of population VI cells were seeded (Fig. 5C). These data indicate that the *in vitro* differences in early osteoclast formation using mixed populations of BMMs are due to differences in osteoclast precursor populations.

4. Discussion

Inflammation and bone loss have long been recognized as intricately connected processes (5, 7, 8, 20, 21). Certain inflammatory factors, including those belonging to the IL-17 cytokine family, have emerged as key drivers of osteoclastic bone resorption through direct and indirect mechanisms (12–15, 22). The ubiquitously expressed IL-17ra forms complexes with other IL-17 receptors to mediate interactions with multiple members of the IL-17 cytokine family. Prior research has primarily focused on IL-17a, which has been reported to be present in sera from healthy humans and mice with concentrations increasing in response to infection, disease, and injury (23–26). In our study of young, unchallenged mice, IL-17a was detected in the sera at similar concentrations in both control and IL-17ra conditional knockout mice, indicating a basal level of IL-17a under homeostatic conditions. High levels of IL-17a have been associated with bone loss in rheumatoid arthritis and in models of post-menopausal bone loss (27–30). Furthermore, systemically targeting IL-17a using an antibody-based approach has been reported to prevent ovariectomy-induced bone loss (12, 31, 32). These studies revealed that IL-17 signaling is an important contributor to tipping the balance between bone formation and bone resorption to favor bone resorbing osteoclasts. Several cells can produce IL-17a, including Th17, natural killer, and γδ T-cells (33, 34). Therefore, the present study sought to further clarify the osteoclast precursor-specific role of IL-17ra signaling in the context of bone homeostasis.

IL-17ra forms receptor complexes with IL-17rc, IL-17rd, IL-17rb, IL-17re to transduce signals from various IL-17 cytokines (35, 36). In immortalized RAW 264.7 pre-osteoclast cells *IL-17ra* and *IL-17rc* are expressed; however, other IL-17 receptors were undetectable (14). Our survey of the various IL-17 receptors in primary murine BMMs also show high expression of *IL-17ra* relative to *IL-17rc* and *IL-17rd*, with no detectable expression of *IL-17re* and *IL-17rb*. This led us to conditionally delete the *IL-17ra* receptor in pre-osteoclasts using the *LysM-Cre* model system. Deletion of *IL-17ra* in osteoclast precursors led to a significant increase in trabecular bone in the femur and the vertebral body. We attribute this increase in bone microstructure to decreased osteoclast formation and

activity from pre-osteoclasts lacking IL-17ra, which was observed *in vivo* and early *in vitro*. Interestingly, two distinct studies using the global knockout (IL-17ra$^{-/-}$) mice did not observe a bone phenotype under homeostatic conditions (12, 24). However, when high turnover was induced by ovariectomy, these studies reported discrepant phenotypes for IL-17ra$^{-/-}$ mice. The initial study reported that IL-17ra$^{-/-}$ exacerbated ovariectomy-induced bone loss (24). Whereas a subsequent study reported that IL-17ra$^{-/-}$ protected against estrogen-deficiency bone loss by inhibiting osteoclastic bone resorption (12). The authors of the latter attributed this discrepancy to the evaluation methods used (i.e., DEXA versus microCT) (12). Importantly, these two reports on global knockout mice demonstrated that IL-17ra has an enigmatic role in bone turnover. It can also be argued that the use of global knockout mice in these prior studies did not allow for the identification of osteoclast- versus osteoblast-specific contributions of IL-17ra signaling to bone turnover. Our study addressed this gap by specifically employing a conditional deletion of IL-17ra approach to demonstrate that absence of IL-17ra signaling in pre-osteoclasts can increase bone mass; thereby, confirming the importance of this inflammatory cytokine receptor in promoting bone resorption. Future studies focusing on conditional deletion of IL-17ra in osteoblasts are likely to be equally informative.

IL-17ra has been previously reported to modulate monocyte subsets *in vivo* (37). We therefore surveyed different osteoclast precursor populations within the bone marrow compartment to determine if deletion of IL-17ra in LysM+ cells would influence preosteoclast abundance. Our analyses demonstrated that conditional deletion of IL-17ra significantly decreased the abundance of population IV and population VI osteoclast progenitors in freshly isolated bone marrow. The low abundance of this highly osteoclastogenic populations in the IL-17ra cKO mice provides some mechanistic insight into the lower osteoclast numbers and activity observed *in vivo*. Furthermore, when we cultured an equal number of population VI osteoclast progenitors from sorted bone marrow the *in vitro* differences in osteoclast formation at day 3 were no longer observed. These data indicate that in the absence of IL-17ra, the osteoclast precursor pool is altered *in vivo* which likely contributed to the lower number of osteoclasts formed using a heterogenous population of bone marrow cells observed *in vitro* and the *in vivo* reduced osteoclast phenotype. Collectively, these data suggest that activation of IL-17ra signaling elicits a basal effect on myeloid cell differentiation in the absence of injury or infection. Future research should focus on the signaling pathways and effectors downstream of IL-17ra responsible for these differences in osteoclast progenitor populations.

IL-17ra facilitates the cellular responses to a majority of the IL-17 cytokine family, including IL-17a, IL-17c, IL-17f, and IL-17e (35, 38). Based on our gene expression data of other IL-17 receptors in osteoclast precursors, it is likely that either IL-17a, IL-17f, or IL-17a/f heterodimer are responsible for these effects. Little is known regarding the influence of IL-17f on osteoclastogenesis; however, the role of IL-17a has received much more attention with conflicting reports. IL-17a has been reported to inhibit (14, 39), induce (11, 13, 22), and not affect (12) osteoclastogenesis. These discrepancies may be due to concentration-dependent or cell-dependent (i.e., immortalized versus primary cells) differences. Low concentrations of IL-17a have been reported to induce osteoclast formation, whereas high concentrations can inhibit osteoclastogenesis. Moreover, certain

osteoclast precursor populations have been reported to respond differently to IL-17a (15). Future work will need to be undertaken to decipher which IL-17ra agonists and precise downstream signaling pathways that mediate these effects.

In summary, we report that conditional deletion of *IL-17ra* in osteoclast precursors leads to higher trabecular bone mass in mice. This phenotype stemmed from decreased osteoclast number and activity, which was likely a result of decreased osteoclast precursor abundance. Collectively, our study identifies IL-17ra as a potential therapeutic target to increase bone mass, which may be targeted using antibody-based approaches such as the FDA-approved antibody brodalumab.

Supplementary Material

Refer to Web version on PubMed Central for supplementary material.

Funding:

This work was supported by the National Institutes of Health (R01 AG064464), Veterans Health Administration (I01BX004708), and Emory University.

References

1. Wiktor-Jedrzejczak W, Bartocci A, Ferrante AW Jr., Ahmed-Ansari A, Sell KW, Pollard JW, Stanley ER. Total absence of colony-stimulating factor 1 in the macrophage-deficient osteopetrotic (op/op) mouse. Proc Natl Acad Sci U S A. 1990;87(12):4828–32. Epub 1990/06/01. doi: 10.1073/pnas.87.12.4828. [PubMed: 2191302]
2. Anderson DM, Maraskovsky E, Billingsley WL, Dougall WC, Tometsko ME, Roux ER, Teepe MC, DuBose RF, Cosman D, Galibert L. A homologue of the TNF receptor and its ligand enhance T-cell growth and dendritic-cell function. Nature. 1997;390(6656):175–9. Epub 1997/11/21. doi: 10.1038/36593. [PubMed: 9367155]
3. Maeda K, Kobayashi Y Fau - Udagawa N Udagawa N Fau - Uehara S, Uehara S Fau - Ishihara A, Ishihara A Fau - Mizoguchi T, Mizoguchi T Fau - Kikuchi Y, Kikuchi Y Fau - Takada I, Takada I Fau - Kato S, Kato S Fau - Kani S, Kani S Fau - Nishita M, Nishita M Fau - Marumo K, Marumo K Fau - Martin TJ, Martin Tj Fau - Minami Y, Minami Y Fau - Takahashi N, Takahashi N. Wnt5a-Ror2 signaling between osteoblast-lineage cells and osteoclast precursors enhances osteoclastogenesis. Nature Medicine. 2012(1546–170X (Electronic)).
4. Chen X, Wang Z, Duan N, Zhu G, Schwarz EM, Xie C. Osteoblast-osteoclast interactions. Connect Tissue Res. 2018;59(2):99–107. Epub 2017/03/23. doi: 10.1080/03008207.2017.1290085. [PubMed: 28324674]
5. Graves DT, Li J, Cochran DL. Inflammation and uncoupling as mechanisms of periodontal bone loss. J Dent Res. 2011;90(2):143–53. Epub 2010/12/08. doi: 10.1177/0022034510385236. [PubMed: 21135192]
6. Roberts JL, Liu G, Paglia DN, Kinter CW, Fernandes LM, Lorenzo J, Hansen MF, Arif A, Drissi H. Deletion of Wnt5a in osteoclasts results in bone loss through decreased bone formation. Ann N Y Acad Sci. 2020. Epub 2020/01/11. doi: 10.1111/nyas.14293.
7. Bertolini DR, Nedwin GE, Bringman TS, Smith DD, Mundy GR. Stimulation of bone resorption and inhibition of bone formation in vitro by human tumour necrosis factors. Nature. 1986;319(6053):516–8. Epub 1986/02/06. doi: 10.1038/319516a0. [PubMed: 3511389]
8. Nguyen L, Dewhirst FE, Hauschka PV, Stashenko P. Interleukin-1 beta stimulates bone resorption and inhibits bone formation in vivo. Lymphokine Cytokine Res. 1991;10(1–2):15–21. Epub 1991/04/01. [PubMed: 1873357]

9. Lam J, Takeshita S, Barker JE, Kanagawa O, Ross FP, Teitelbaum SL. TNF-alpha induces osteoclastogenesis by direct stimulation of macrophages exposed to permissive levels of RANK ligand. J Clin Invest. 2000;106(12):1481–8. Epub 2000/12/20. doi: 10.1172/JCI11176. [PubMed: 11120755]
10. Wei S, Kitaura H, Zhou P, Ross FP, Teitelbaum SL. IL-1 mediates TNF-induced osteoclastogenesis. J Clin Invest. 2005;115(2):282–90. Epub 2005/01/26. doi: 10.1172/JCI23394. [PubMed: 15668736]
11. Scheffler JM, Grahnemo L, Engdahl C, Drevinge C, Gustafsson KL, Corciulo C, Lawenius L, Iwakura Y, Sjogren K, Lagerquist MK, Carlsten H, Ohlsson C, Islander U. Interleukin 17A: a Janus-faced regulator of osteoporosis. Sci Rep. 2020;10(1):5692. Epub 2020/04/02. doi: 10.1038/s41598-020-62562-2. [PubMed: 32231224]
12. DeSelm CJ, Takahata Y, Warren J, Chappel JC, Khan T, Li X, Liu C, Choi Y, Kim YF, Zou W, Teitelbaum SL. IL-17 mediates estrogen-deficient osteoporosis in an Act1-dependent manner. J Cell Biochem. 2012;113(9):2895–902. Epub 2012/04/19. doi: 10.1002/jcb.24165. [PubMed: 22511335]
13. Adamopoulos IE, Chao C-c, Geissler R, Laface D, Blumenschein W, Iwakura Y, McClanahan T, Bowman EP. Interleukin-17A upregulates receptor activator of NF-κB on osteoclast precursors. Arthritis Research & Therapy. 2010;12(1):R29-R. doi: 10.1186/ar2936.
14. Kitami S, Tanaka H, Kawato T, Tanabe N, Katono-Tani T, Zhang F, Suzuki N, Yonehara Y, Maeno M. IL-17A suppresses the expression of bone resorption-related proteinases and osteoclast differentiation via IL-17RA or IL-17RC receptors in RAW264.7 cells. Biochimie. 2010;92(4):398–404. Epub 2010/01/05. doi: 10.1016/j.biochi.2009.12.011. [PubMed: 20045440]
15. Sprangers S, Schoenmaker T, Cao Y, Everts V, de Vries TJ. Different Blood-Borne Human Osteoclast Precursors Respond in Distinct Ways to IL-17A. J Cell Physiol. 2016;231(6):1249–60. Epub 2015/10/23. doi: 10.1002/jcp.25220. [PubMed: 26491867]
16. Wang K, Kim MK, Di Caro G, Wong J, Shalapour S, Wan J, Zhang W, Zhong Z, Sanchez-Lopez E, Wu LW, Taniguchi K, Feng Y, Fearon E, Grivennikov SI, Karin M. Interleukin-17 receptor a signaling in transformed enterocytes promotes early colorectal tumorigenesis. Immunity. 2014;41(6):1052–63. Epub 2014/12/20. doi: 10.1016/j.immuni.2014.11.009. [PubMed: 25526314]
17. Bouxsein ML, Boyd SK, Christiansen BA, Guldberg RE, Jepsen KJ, Müller R. Guidelines for assessment of bone microstructure in rodents using micro–computed tomography. Journal of Bone and Mineral Research. 2010;25(7):1468–86. doi: 10.1002/jbmr.141. [PubMed: 20533309]
18. Soung DY, Talebian L, Matheny CJ, Guzzo R, Speck ME, Lieberman JR, Speck NA, Drissi H. Runx1 dose-dependently regulates endochondral ossification during skeletal development and fracture healing. Journal of Bone and Mineral Research. 2012;27(7):1585–97. doi: 10.1002/jbmr.1601. [PubMed: 22431360]
19. Jacquin C, Gran DE, Lee SK, Lorenzo JA, Aguila HL. Identification of multiple osteoclast precursor populations in murine bone marrow. J Bone Miner Res. 2006;21(1):67–77. Epub 2005/12/16. doi: 10.1359/JBMR.051007. [PubMed: 16355275]
20. Cao JJ, Wronski TJ, Iwaniec U, Phleger L, Kurimoto P, Boudignon B, Halloran BP. Aging increases stromal/osteoblastic cell-induced osteoclastogenesis and alters the osteoclast precursor pool in the mouse. J Bone Miner Res. 2005;20(9):1659–68. Epub 2005/08/02. doi: 10.1359/JBMR.050503. [PubMed: 16059637]
21. Chung PL, Zhou S, Eslami B, Shen L, LeBoff MS, Glowacki J. Effect of age on regulation of human osteoclast differentiation. J Cell Biochem. 2014;115(8):1412–9. Epub 2014/04/05. doi: 10.1002/jcb.24792. [PubMed: 24700654]
22. Song L, Tan J, Wang Z, Ding P, Tang Q, Xia M, Wei Y, Chen L. Interleukin17A facilitates osteoclast differentiation and bone resorption via activation of autophagy in mouse bone marrow macrophages. Mol Med Rep. 2019;19(6):4743–52. Epub 2019/05/07. doi: 10.3892/mmr.2019.10155. [PubMed: 31059030]
23. Li Q, Ding S, Wang YM, Xu X, Shen Z, Fu R, Liu M, Hu C, Zhang C, Cao Q, Wang Y. Age-associated alteration in Th17 cell response is related to endothelial cell senescence and atherosclerotic cerebral infarction. Am J Transl Res. 2017;9(11):5160–8. Epub 2017/12/09. [PubMed: 29218113]

24. Goswami J, Hernández-Santos N, Zuniga LA, Gaffen SL. A Bone-Protective Role for IL-17 Receptor Signaling in Ovariectomy-Induced Bone Loss. European journal of immunology. 2009;39(10):2831–9. doi: 10.1002/eji.200939670. [PubMed: 19731364]
25. Tang X. Analysis of interleukin-17 and interleukin-18 levels in animal models of atherosclerosis. Exp Ther Med. 2019;18(1):517–22. Epub 2019/07/10. doi: 10.3892/etm.2019.7634. [PubMed: 31281442]
26. Techatanawat S, Surarit R, Chairatvit K, Khovidhunkit W, Roytrakul S, Thanakun S, Kobayashi H, Khovidhunkit SP, Izumi Y. Salivary and serum interleukin-17A and interleukin-18 levels in patients with type 2 diabetes mellitus with and without periodontitis. PLoS One. 2020;15(2):e0228921. Epub 2020/02/14. doi: 10.1371/journal.pone.0228921.
27. Le Goff B, Bouvard B, Lequerre T, Lespessailles E, Marotte H, Pers YM, Cortet B. Implication of IL-17 in Bone Loss and Structural Damage in Inflammatory Rheumatic Diseases. Mediators Inflamm. 2019;2019:8659302. Epub 2019/09/06. doi: 10.1155/2019/8659302.
28. Bhadricha H, Patel V, Singh AK, Savardekar L, Patil A, Surve S, Desai M. Increased frequency of Th17 cells and IL-17 levels are associated with low bone mineral density in postmenopausal women. Sci Rep. 2021;11(1):16155. Epub 2021/08/11. doi: 10.1038/s41598-021-95640-0.
29. Molnar I, Bohaty I, Somogyine-Vari E. High prevalence of increased interleukin-17A serum levels in postmenopausal estrogen deficiency. Menopause. 2014;21(7):749–52. Epub 2013/11/21. doi: 10.1097/GME.0000000000000125. [PubMed: 24253487]
30. Gumus P, Buduneli E, Biyikoglu B, Aksu K, Sarac F, Nile C, Lappin D, Buduneli N. Gingival crevicular fluid, serum levels of receptor activator of nuclear factor-kappaB ligand, osteoprotegerin, and interleukin-17 in patients with rheumatoid arthritis and osteoporosis and with periodontal disease. J Periodontol. 2013;84(11):1627–37. Epub 2013/01/19. doi: 10.1902/jop.2013.120595. [PubMed: 23327689]
31. Tyagi AM, Srivastava K, Mansoori MN, Trivedi R, Chattopadhyay N, Singh D. Estrogen deficiency induces the differentiation of IL-17 secreting Th17 cells: a new candidate in the pathogenesis of osteoporosis. PLoS One. 2012;7(9):e44552. Epub 2012/09/13. doi: 10.1371/journal.pone.0044552.
32. Tyagi AM, Mansoori MN, Srivastava K, Khan MP, Kureel J, Dixit M, Shukla P, Trivedi R, Chattopadhyay N, Singh D. Enhanced immunoprotective effects by anti-IL-17 antibody translates to improved skeletal parameters under estrogen deficiency compared with anti-RANKL and anti-TNF-alpha antibodies. J Bone Miner Res. 2014;29(9):1981–92. Epub 2014/03/29. doi: 10.1002/jbmr.2228. [PubMed: 24677326]
33. Ouyang X, Yang Z, Zhang R, Arnaboldi P, Lu G, Li Q, Wang W, Zhang B, Cui M, Zhang H, Liang-Chen J, Qin L, Zheng F, Huang B, Xiong H. Potentiation of Th17 cytokines in aging process contributes to the development of colitis. Cell Immunol. 2011;266(2):208–17. Epub 2010/11/16. doi: 10.1016/j.cellimm.2010.10.007. [PubMed: 21074754]
34. De Angulo A, Faris R, Daniel B, Jolly C, deGraffenried L. Age-related increase in IL-17 activates pro-inflammatory signaling in prostate cells. Prostate. 2015;75(5):449–62. Epub 2015/01/07. doi: 10.1002/pros.22931. [PubMed: 25560177]
35. Wright JF, Bennett F, Li B, Brooks J, Luxenberg DP, Whitters MJ, Tomkinson KN, Fitz LJ, Wolfman NM, Collins M, Dunussi-Joannopoulos K, Chatterjee-Kishore M, Carreno BM. The human IL-17F/IL-17A heterodimeric cytokine signals through the IL-17RA/IL-17RC receptor complex. J Immunol. 2008;181(4):2799–805. Epub 2008/08/08. doi: 10.4049/jimmunol.181.4.2799. [PubMed: 18684971]
36. Gaffen SL. An overview of IL-17 function and signaling. Cytokine. 2008;43(3):402–7. Epub 2008/08/15. doi: 10.1016/j.cyto.2008.07.017. [PubMed: 18701318]
37. Ge S, Hertel B, Susnik N, Rong S, Dittrich AM, Schmitt R, Haller H, von Vietinghoff S. Interleukin 17 receptor A modulates monocyte subsets and macrophage generation in vivo. PLoS One. 2014;9(1):e85461. Epub 2014/01/24. doi: 10.1371/journal.pone.0085461.
38. McGeachy MJ, Cua DJ, Gaffen SL. The IL-17 Family of Cytokines in Health and Disease. Immunity. 2019;50(4):892–906. Epub 2019/04/18. doi: 10.1016/j.immuni.2019.03.021. [PubMed: 30995505]
39. Nosaka K, Inoue H, Hirano S-i, Uchihashi K, Nishikawa Y. IL-17A inhibits osteoclast differentiation of RANKL-stimulated RAW264.7 cells by suppressing JNK phosphorylation

and c-Fos expression. Journal of Osaka Dental University. 2014;48(2):117–23. doi: 10.18905/jodu.48.2_117.

- Conditional deletion of IL-17ra in LysM+ osteoclast precursors increases trabecular bone mass in young, unchallenged mice
- IL-17ra deletion in pre-osteoclasts decreases osteoclast number and activity in vivo
- Conditional deletion of IL-17ra decreases the abundance of bone marrow-derived osteoclast progenitor populations

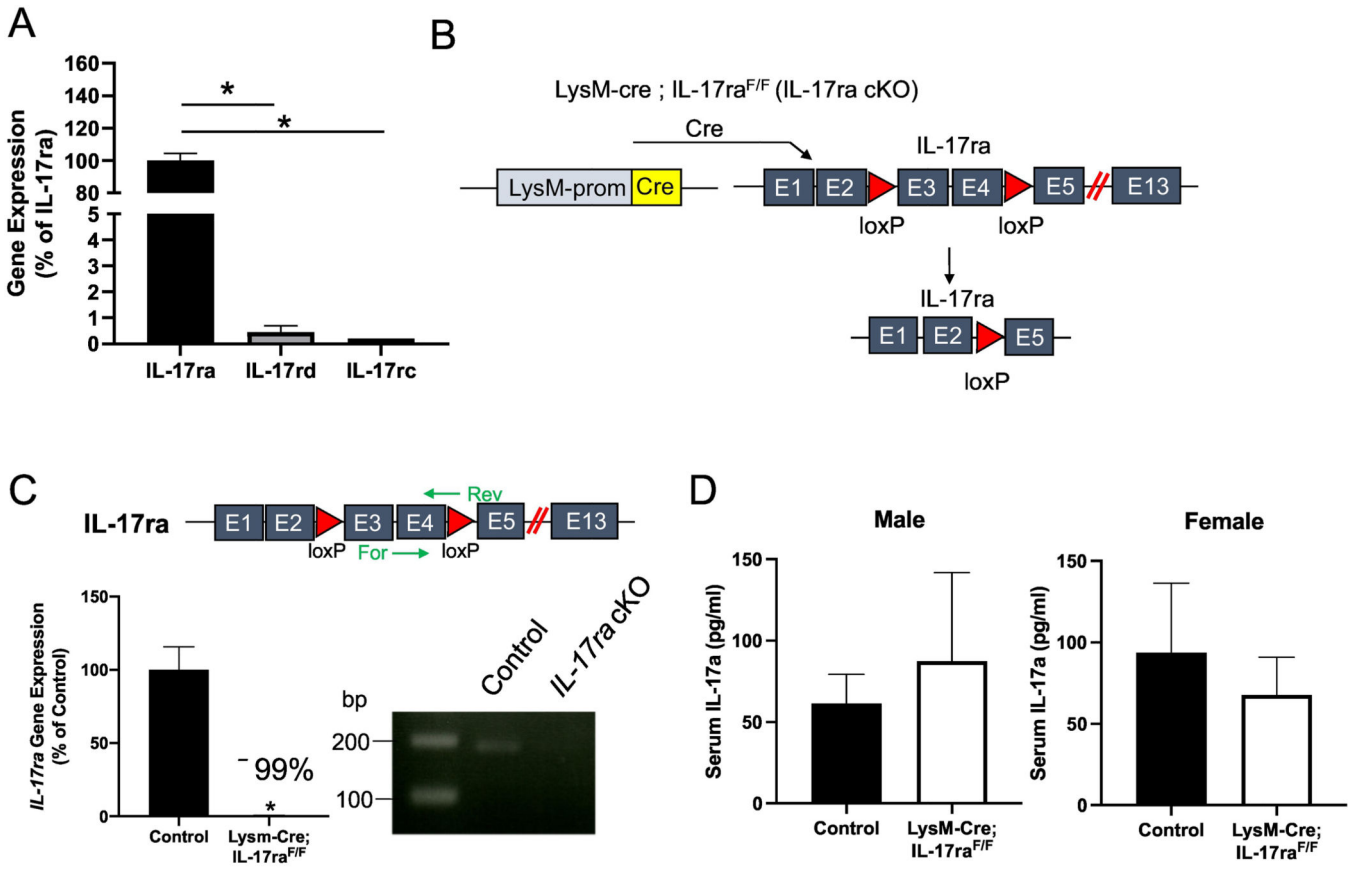

Figure 1: *IL-17ra* is highly expressed in osteoclast precursors.

(**A**) A survey of IL-17 receptors shows high expression of *IL-17ra* in osteoclast precursors, with significantly lower expression of *IL-17c* and *IL-17d*. (**B**) *IL-17ra* cKO mice were generated by crossing *LysM-Cre* mice with *IL-17ra*$^{F/F}$ mice. Cre-mediated recombination in osteoclast precursors results in excision of exon 3 and 4. (**C**) BMMs were isolated from 10-week old mice and cultured in the presence of M-CSF (30 ng/ml) for 3 days. *LysM-Cre* resulted in a significant decrease in *IL-17ra* gene expression by using primers that amplify the excised region of *IL-17ra*. Agarose gel image of qPCR product confirms the decrease in *IL-17ra* gene expression. (**D**) Serum IL-17a levels were not different between control and IL-17ra cKO mice. Abbreviations: cKO, conditional knockout; M-CSF, macrophage colony stimulating factor; RANKL, receptor activator of nuclear factor kappa-B ligand. Data represent mean ± SD. * $P < 0.05$.

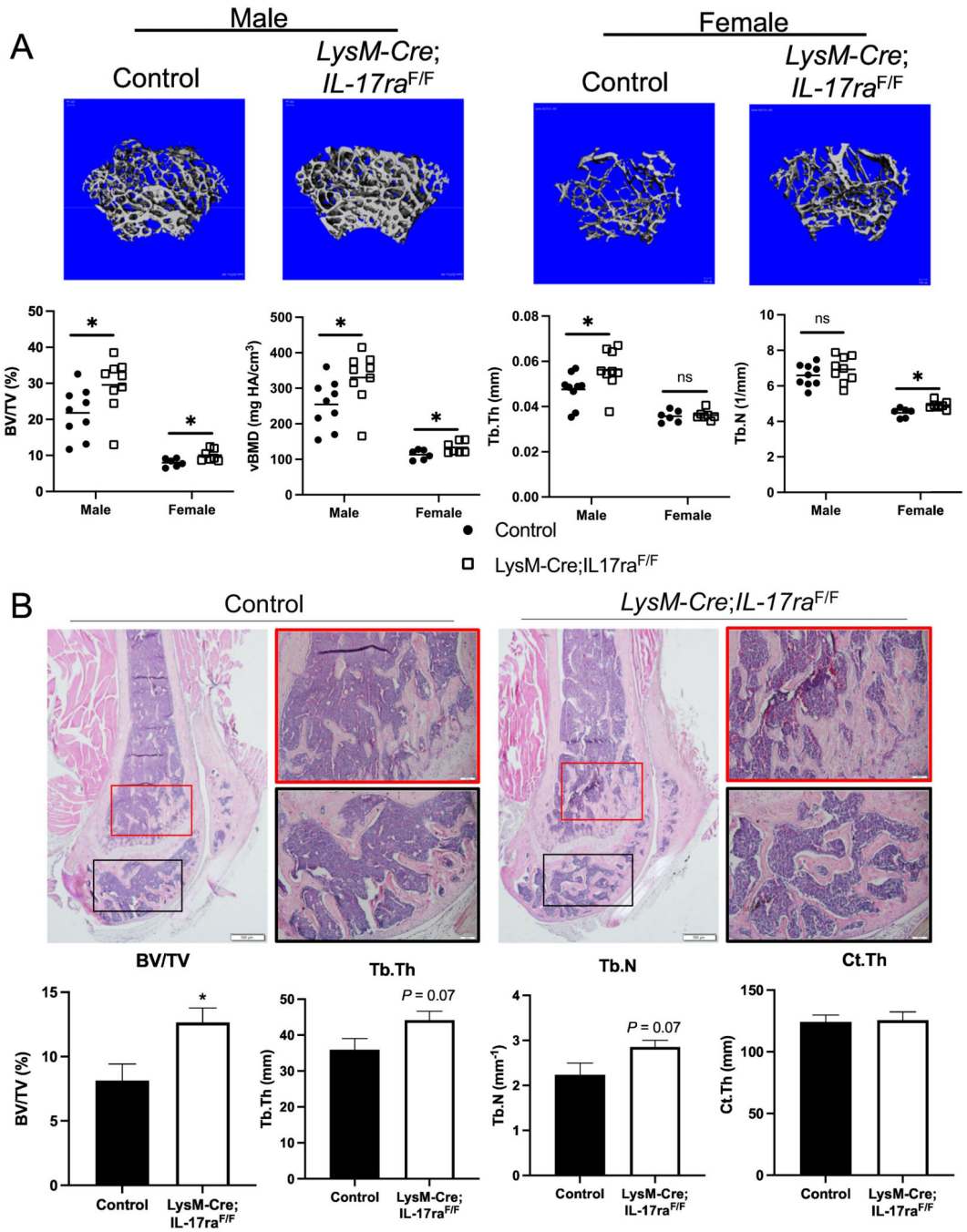

Figure 2: Increased femur cancellous bone in *IL-17ra* cKO mice.

(**A**) Deletion of IL-17ra in osteoclast precursors significantly increased femur trabecular BV/TV, vBMD, and Tb.Th in male mice. In female mice, IL-17ra cKO increased BV/TV, vBMD, and Tb.N. (**B**) Static histomorphometric analyses of femur trabecular bone shows increased BV/TV. Representative histological images (2x and 10x). Abbreviations: BV/TV, bone volume fraction; vBMD, volumetric bone mineral density; Tb.Th, trabecular thickness; Tb.N, trabecular number; Ct.Th, cortical thickness. Data represent mean ± SD, * $P < 0.05$.

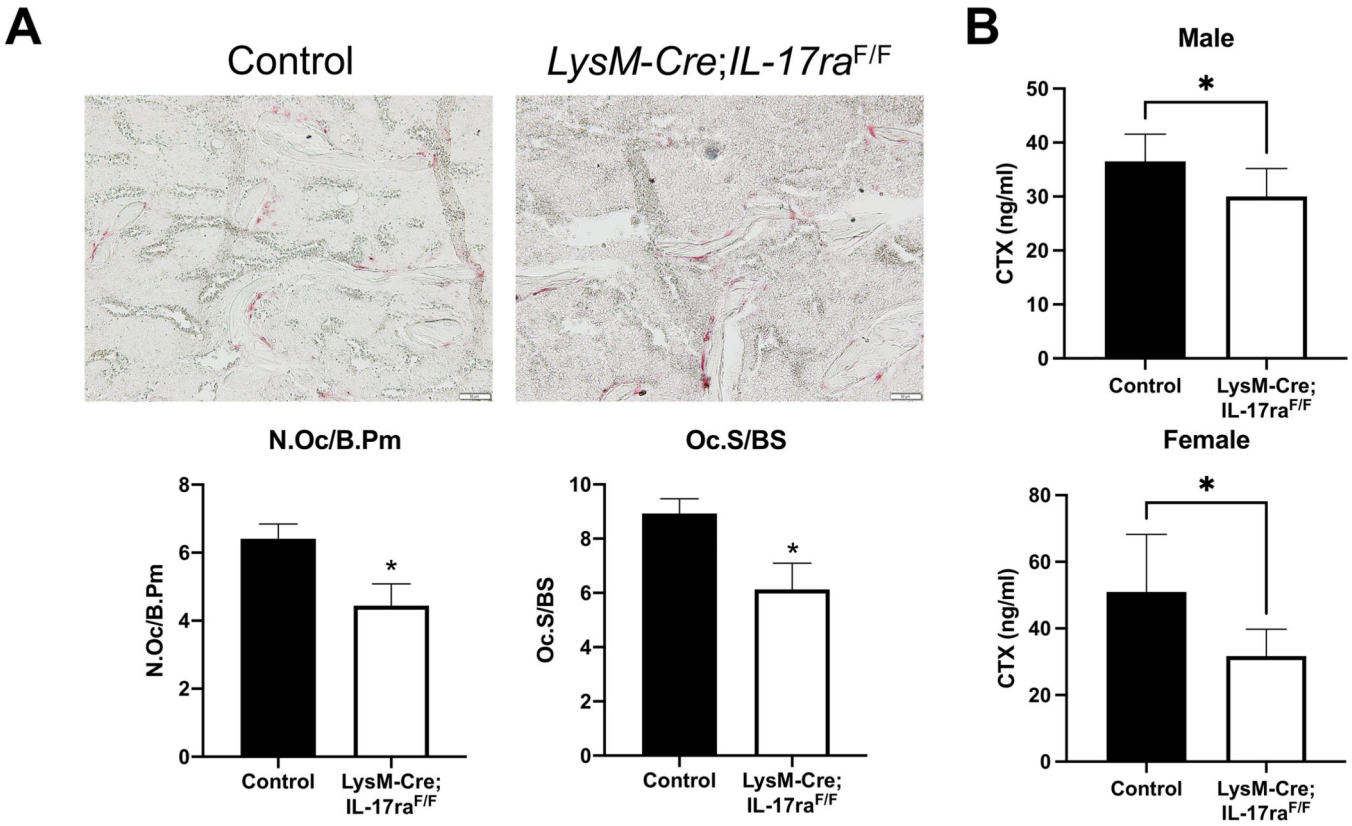

Figure 3: Deletion of *IL-17ra* in preosteoclasts decreases osteoclast number and activity.

(**A**) Static histomorphometric quantification of osteoclasts showed decreased osteoclast number and surface in male IL-17ra cKO mice. N.Oc/B.Pm, number of osteoclasts over bone perimeter; Oc.S/BS, osteoclast surface over bone surface. (**B**) Sera levels of CTX were significantly lower in male and female IL-17ra cKO mice. Data represent mean ± SD, * $P < 0.05$

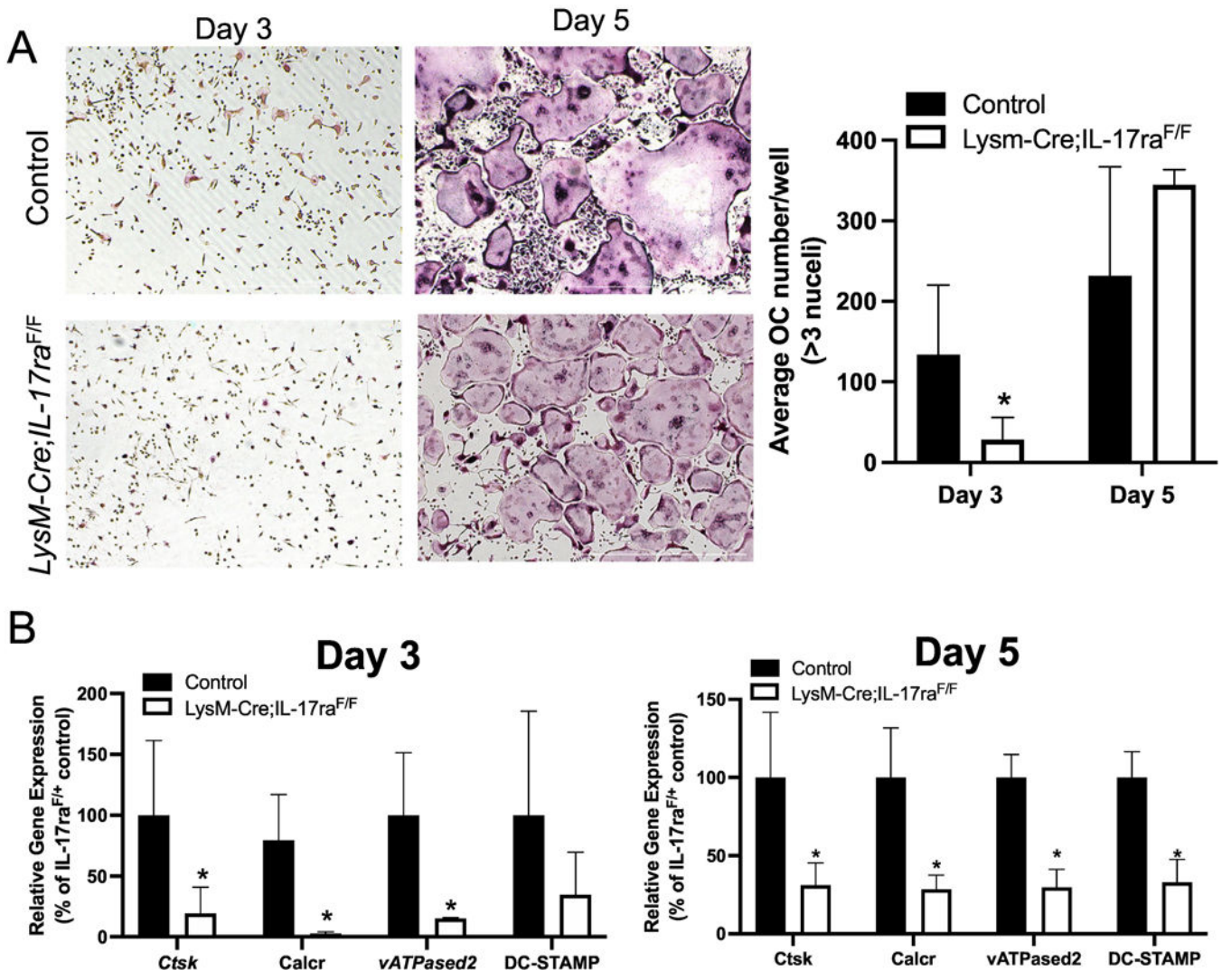

Figure 4: Deletion of *IL-17a* in osteoclast precursors impairs osteoclast differentiation.

(**A**) BMMs from 10-week old male mice were treated with M-CSF (30ng/ml) and RANKL (50 ng/ml) for 3 and 5 days. BMMs isolated from *IL-17ra* cKO formed fewer osteoclasts compared to control at day 3. No differences in osteoclast numbers were observed at day 5. (**B**) *IL-17ra* cKO led to significantly lower expression of *Ctsk*, *Calcr*, and vATPased2 at day 3 and significantly lower expression of *Ctsk*, *Calcr*, vATPased2, and DC-Stamp at day 5. Abbreviations: cKO, conditional knockout; OC, osteoclast. Data represent mean ± SD. * $P < 0.05$.

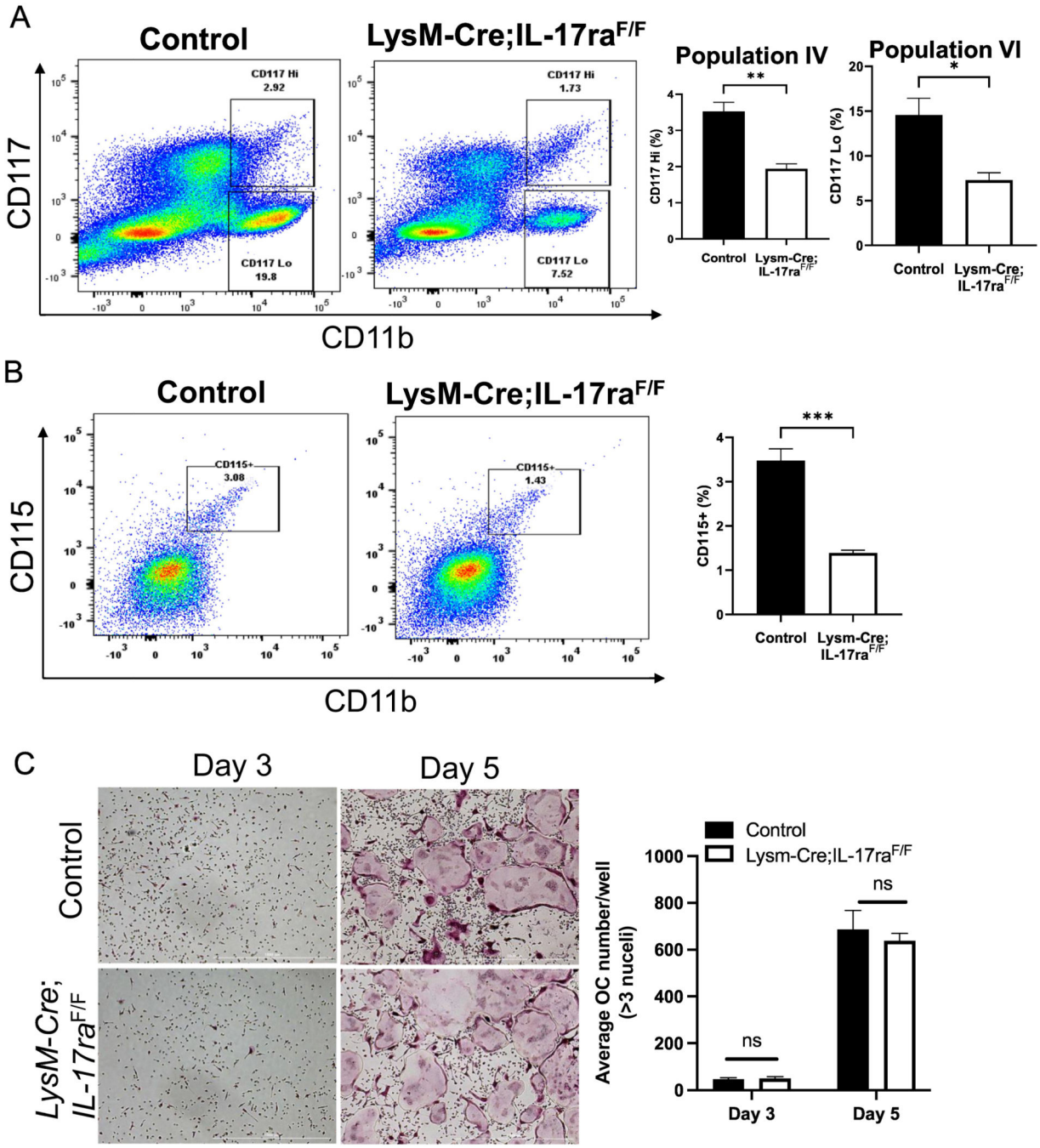

Figure 5: *IL-17ra* cKO alters bone marrow osteoclast precursor abundance.

(**A**) Flow cytometry plots showing the dissection of bone marrow osteoclast precursors populations. Population IV (CD117 ^{high}) and population VI (CD117 ^{low}) were significantly lower in the bone marrow of *IL-17ra* conditional knockout mice. (**B**) Flow cytometry plots showing the dissection of bone marrow osteoclast precursors populations shows significantly lower CD115+ osteoclast progenitors in the *IL-17ra* conditional knockout mice. (**C**) No

significant differences in osteoclast formation when equal numbers of sorted population VI osteoclast precursors were cultured for 3 and 5 days. Data represent mean ± SD, * $P < 0.05$